Earth Syst. Sci. Data Discuss., doi:10.5194/essd-2015-43, 2016
Manuscript under review for journal Earth Syst. Sci. Data
Published: 19 January 2016

Open Access Earth System Science Data Discussions

A new global interior ocean mapped climatology: the 1ºx1º GLODAP version 2

Siv K. Lauvset[1,2]*, Robert M. Key[3], Are Olsen[1,2], Steven van Heuven[4], Anton Velo[5], Xiaohua Lin[3], Carsten Schirnick[6], Alex Kozyr[7], Toste Tanhua[6], Mario Hoppema[8], Sara Jutterström[9], Reiner Steinfeldt[10], Emil Jeansson[2], Masao Ishii[11], Fiz F. Perez[5], Toru Suzuki[12], Sylvain Watelet[13].

[1]Geophysical Institute, University of Bergen and Bjerknes Centre for Climate Research, Allègaten 70, 5007 Bergen, Norway

[2]Uni Research Climate, Bjerknes Centre for Climate Research, Allegt. 55, 5007 Bergen, Norway

[3]Atmospheric and Oceanic Sciences, Princeton University, 300 Forrestal Road, Sayre Hall, Princeton, NJ 08544, USA

[4]Royal Netherlands Institute for Sea Research (NIOZ), Marine Geology and Chemical Oceanography, P.O. Box 59, 1790 AB Den Burg, The Netherlands

[5]Instituto de Investigaciones Marinas - CSIC, Eduardo Cabello 6, 36208 Vigo, Spain

[6]GEOMAR Helmholtz Centre for Ocean Research Kiel, Düsternbrooker Weg 20, 24105 Kiel, Germany

[7]Carbon Dioxide Information Analysis Center, Environmental Sciences Division, Oak Ridge National Laboratory, U.S. Department of Energy, Building 4500N, Mail Stop 6290, Oak Ridge, TN 37831-6290, U.S.A.

[8]Alfred Wegener Institute Helmholtz Centre for Polar and Marine Research, Bussestrasse 24, 27570 Bremerhaven, Germany

[9]IVL Swedish Environmental Research Institute, Ascheberggatan 44, 411 33 Göteborg, Sweden

[10]University of Bremen, Institute of Environmental Physics, Otto-Hahn-Allee, 28359 Bremen, Germany

[11]Oceanography and Geochemistry Research Department, Meteorological Research Institute, Japan Meteorological Agency, 1-1 Nagamine, Tsukuba, 305-0052 Japan

[12]Marine Information Research Center, Japan Hydrographic Association, 1-6-6-6F, Hanedakuko, Otaku, Tokyo, 144-0041 Japan

[13]Department of Astrophysics, Geophysics and Oceanography, University of Liège, Liège, Belgium

*Communication to Siv K. Lauvset (siv.lauvset@uib.no)

Earth Syst. Sci. Data Discuss., doi:10.5194/essd-2015-43, 2016
Manuscript under review for journal Earth Syst. Sci. Data
Published: 19 January 2016

Open Access Earth System Science Data Discussions

Abstract

We here present the new GLODAP version 2 (GLODAPv2) mapped climatology, which is based on data from all ocean basins up to and including 2013. In contrast to its predecessor, GLODAPv1.1, this climatology also covers the Arctic Ocean and Mediterranean Sea. The quality controlled and internally consistent data product files of GLODAPv2 (Olsen et al., 2015; Key et al., 2015) were used to create global 1ºx1º mapped climatologies of total dissolved inorganic carbon, total alkalinity, and pH using the Data-Interpolating Variational Analysis (DIVA) mapping method. Climatologies were created for 33 standard pressure surfaces. To minimize the risk of translating temporal variability in the input data to spatial variations in the mapped climatologies, layers with pressures of 1000 dbar, or less, were mapped for two different time periods: 1986-1999 and 2000-2013, roughly corresponding to the "WOCE" and "CLIVAR" eras of global ocean surveys. All data from the 1972-2013 period were used in the mapping of pressures higher than 1000 dbar. In addition to the marine CO_2 chemistry parameters listed above, nitrate, phosphate, silicate, oxygen, salinity and theta were also mapped using DIVA. For these parameters all data from the full 1972-2013 period were used on all 33 surfaces. The GLODAPv2 global 1ºx1º mapped climatologies, including error fields and ancillary information have been made available at the GLODAPv2 web page at the Carbon Dioxide Information Analysis Center (CDIAC, http://cdiac.ornl.gov/oceans/GLODAPv2/).

1 Introduction

Accurate estimates of recent changes in the ocean carbon cycle, including how these changes will influence climate, requires high quality data. The fully quality controlled and internally consistent Global Ocean Data Analysis Project (GLODAPv1.1, Key et al., 2004) has for the past decade been the only global interior ocean carbon data product available. GLODAPv1.1 has been and continues to be of immense value to the ocean scientific community, which is reflected in the almost 500 scientific studies that have used and cited GLODAPv1.1 so far. GLODAPv1.1 has been used most prominently for calculation of the global ocean inventory for anthropogenic CO_2 by *e.g.* Sabine et al. (2004) and for validation of global biogeochemical or earth system models by *e.g.* Bopp et al. (2013).

The GLODAPv1.1 data product is dominated by data from the World Ocean Circulation Experiment (WOCE) survey of the 1990s, but contains data from the entire period

Earth Syst. Sci. Data Discuss., doi:10.5194/essd-2015-43, 2016
Manuscript under review for journal Earth Syst. Sci. Data
Published: 19 January 2016

1972-1999, though very few data north of 60ºN in the Atlantic and no data in the Arctic Ocean or Mediterranean Sea. Many more seawater CO_2 chemistry data have been collected at research cruises after 1999, particularly within the framework of the global repeat hydrography program CLIVAR/GO-SHIP (Feely et al., 2014; Talley et al. 2016) so that significantly more interior ocean carbon data exists today than was available in 2004.

In response to the shortcomings of GLODAPv1.1 and to include more recent data, the updated and expanded version GLODAPv2 (Key et al., 2015; Olsen et al., 2015), has been developed. This new data product combines GLODAPv1.1 with data from the two recent regional synthesis products: Carbon in Atlantic Ocean (CARINA, Key et al., 2010); and Pacific Ocean Interior Carbon (PACIFICA, Suzuki et al., 2013). In addition, data from 168 cruises not previously included in any of these data products—both new and historical—have been included. Notably, 116 cruises in GLODAPv2 cover the Arctic Mediterranean Seas, *i.e.*, the Arctic Ocean and the Nordic Seas (>65ºN). GLODAPv2 data are available in three forms: as original, unadjusted data from each cruise in WOCE exchange format files; as a merged and calibrated data product, where adjustments have been applied to minimize measurement biases and several calculated data have been added to complete the data coverage; and as a mapped climatology. This paper presents the methods used for creating the mapped climatology and its main features, while the assembly of the data and construction of the product, including the broad features and output of the secondary quality control are described by Olsen et al. (2015).

As opposed to a gridded data product, which *e.g.* the Surface Ocean CO_2 Atlas (Pfeil et al., 2013; Bakker et al., 2014) provides (Sabine et al., 2013), we have created mapped climatologies. The difference is that gridded data are observations projected onto a grid, using some form of binning and averaging, but no interpolation or other form of calculation is used to fill gaps in the observational record. In mapped data the gaps have been filled, in the case of GLODAPv2 using an objective mathematical method. The method used to create the mapped climatologies from the merged and calibrated data product is presented in Section 2.2. Some of the resulting data fields and their associated error estimates are shown in Section 3 to highlight important features in the data product; and finally some recommendations for use and interpretation are given in Section 4.

Earth Syst. Sci. Data Discuss., doi:10.5194/essd-2015-43, 2016
Manuscript under review for journal Earth Syst. Sci. Data
Published: 19 January 2016

Open Access Earth System Science Data Discussions

2 Methods

2.1 Input data

The input data for the GLODAPv2 mapped climatology consisted of the bias corrected and merged data product from GLODAPv2 (Olsen et al., 2015). Whereas the complete data product contain many variables, we mapped the GLODAPv2 primary biogeochemical variables (Olsen et al., 2015): total dissolved inorganic carbon (TCO_2), total alkalinity (TAlk), pH, saturation state of calcite and aragonite (Ω_C and Ω_A), nitrate (NO_3^-), phosphate (PO_4^{3-}), silicate (Si), dissolved oxygen (O_2), salinity, and potential temperature, where the latter two variables are to be used as a reference for the biogeochemical variables. The GLODAPv2 data product includes vertically interpolated data for the nutrients, oxygen and salinity if any of those were missing from a bottle data-point, and calculated seawater CO_2 chemistry data whenever pairs of measured CO_2 chemistry parameters were available (Olsen et al., 2015). These were all included in the mapping. The following pre-mapping data treatments were carried out:

1. Ω_C and Ω_A were calculated from the TCO_2 and TAlk pair at *in situ* temperature and pressure using the MATLAB version (van Heuven et al., 2009) of CO2SYS (Lewis and Wallace, 1998). We used pressure, temperature, salinity, phosphate, and silicate from the GLODAPv2 data product, the dissociation constants of Lueker et al. (2000) for carbonate, Dickson (1990) for sulphate, and the total borate concentration of Uppstrom (1974).
2. All data were vertically interpolated onto 33 surfaces: 0, 10, 20, 30, 50, 75, 100, 125, 150, 200, 250, 300, 400, 500, 600, 700, 800, 900, 1000, 1100, 1200, 1300, 1400, 1500, 1750, 2000, 2500, 3000, 3500, 4000, 4500, 5000, 5500 dbar. The interpolation was done station by station, using a cubic hermite spline function. This interpolation method is quite robust, but can give unreliable results in a few unusual circumstances. Consequently, if this interpolation gave values more than 1% different from those produced using a simple linear vertical interpolation the linear results were used. We used the maximum distance criteria specified in Table 1 to avoid interpolation over excessive vertical distances between data points. These maximum distance criteria are similar to those used by Key et al. (2004) for GLODAPv1.1. Note that the GLODAPv2 climatologies cover 33 pressure surfaces, which is slightly different from

Earth Syst. Sci. Data Discuss., doi:10.5194/essd-2015-43, 2016
Manuscript under review for journal Earth Syst. Sci. Data
Published: 19 January 2016

the depth surfaces, originally chosen by Levitus and Boyer (1994), used in GLODAPv1.1.

3. The vertically interpolated data for each pressure surface were then gridded by bin-averaging all data in each 1°x1° grid cell. The mapped climatologies are thus based on gridded data. We do this because the repeat hydrography program means that there are several transects in the ocean that have observations at the same points in space at different points in time.
4. GLODAPv2 includes data for the 42 year period 1972-2013 and in this time frame there have been significant changes in pH, TCO_2, and the saturation states, due to increasing atmospheric levels of CO_2 (*e.g.* Orr et al., 2001; Lauvset et al., 2015; Sabine and Tanhua, 2010). Therefore the upper ocean data, here defined as pressure less than, or equal to, 1000 dbar, were separated into two time periods for TCO_2, pH, Ω_C, and Ω_A: 1986-1999 and 2000-2013, roughly corresponding to the WOCE and CLIVAR eras of global hydrography programs. These were then mapped separately to reduce the risk of transforming time trends into spatial variations in the mapped climatologies. No additional corrections were used to account for the seasonal cycle or potential bias due to uneven temporal sampling. Below 1000 dbar, and for all other mapped parameters, all available data from 1972-2013 were used in the mapping. The inherent assumption is that the change in dissolved inorganic carbon and pH below 1000 dbar is negligible. This assumption is further discussed in Section 4.

2.2 Mapping method

The Data-Interpolating Variational Analysis (DIVA) mapping method (Beckers et al., 2014; Troupin et al., 2012) was used to create the mapped climatologies. DIVA is the implementation of the Variational Inverse Method (VIM) of mapping discrete, spatially varying data. A major difference between this and the Optimal Interpolation (OI) method used in GLODAPv1.1 is how topography is handled. DIVA takes the presence of the seabed and land into account during the mapping and gives better results in coastal areas and around islands. In addition, the entire global ocean can be mapped at once, *e.g*, DIVA does not propagate information across narrow land barriers such as the Panama isthmus so there is no need to split the data into ocean regions which are then stitched together to form a global map. Hence, each climatology is a global analysis for the range 180°W to 180°E with a 1°x1° resolution. To ensure that the analysis converges on the boundaries, *i.e.* the dateline and the

Earth Syst. Sci. Data Discuss., doi:10.5194/essd-2015-43, 2016
Manuscript under review for journal Earth Syst. Sci. Data
Published: 19 January 2016

North Pole, the input data were duplicated for 10º on either side of the dateline and for every 30º in a circle around the North Pole (*i.e.*, north of 82.5ºN data in the longitude band 0-30º were duplicated into the 30-60º and so on), before mapping. This removes most discontinuities along these boundaries, but in some cases discontinuities still appear along the North Pole boundary, most notably in the top 125 dbar in the 2000-2013 climatology for TCO_2. Note that this approach creates an artificially large amount of data in the Arctic Ocean, but the spatial patterns in the observations are retained.

Apart from the data, the most important DIVA input parameters are the spatial correlation length scale (CL) and the data signal-to-noise ratio (SNR). The CL defines the characteristic distance over which a data point influences its neighbors. For GLODAPv2 this was defined a priori as 7º for all parameters, except for TCO_2 and pH. In latitude this approximately matches the 750 km north-south CL used for the GLODAPv1.1 mapped climatologies, but is in longitude much smaller than the 1500 km east-west CL used for GLODAPv1.1. For TCO_2, pH, Ω_C, and Ω_A a CL of 10º was used for the two time periods in the top 1000 dbar, and 7º in the deep ocean. This was required because separating these parameters into two time periods significantly reduced the data density (Figure 1), and the smaller CL led to gaps in the climatology. Since the oceans generally tend to mix easier zonally than meridionally, a pseudo-velocity field and advection constraint was used such that the correlation becomes stronger in the east-west direction even though the input CL is the same for both directions (see the DIVA user manual available at http://modb.oce.ulg.ac.be/mediawiki/index.php/Diva_documents for details). Setting the CL is partly a subjective effort, aiming to strike the optimal balance between large values, which tends to smooth the data fields and reduce mapping errors, and small values, which leads to more correct rendering of fronts and other features. We also want to stay within the physical constraints set by ocean dynamics and natural spatial variability. It is possible to optimize CL in DIVA, but this works well only when the data density is reasonably high. The sparse global data distribution in GLODAPv2 gives optimized CL in the order of 25º. Doing a cruise-by-cruise analysis following Jones et al. (2012) to get spatially varying CL is possible, but would leave large gaps. For GLODAPv2 it was therefore decided to use a globally uniform a priori choice since this is the most transparent and easily reproducible.

The SNR defines how representative the observations are for the climatological state. For spatially varying data sets like GLODAPv2, it is the assumed ratio of climatological spatial variability (“signal”) to the short term variability (“noise”) in the data. For the

Earth Syst. Sci. Data Discuss., doi:10.5194/essd-2015-43, 2016
Manuscript under review for journal Earth Syst. Sci. Data
Published: 19 January 2016

GLODAPv2 mapped climatologies the SNR was defined a priori to be 10 (*i.e.* the noise is 10% of the signal), following Key et al. (2004). To understand the importance of SNR, and the reason for a subjective a priori choice, a brief discussion of the differences between interpolation and approximation/analysis is necessary. When interpolating between points in a data set, gaps between data points are filled but the existing points are not replaced. When approximating, a function, *e.g.* a regression line, is applied that describes the original data points to some degree. The resulting approximated data set has new values at every point and is smoother than the interpolated data set. None of the approximated data points exactly match the original ones, and that assumes more uncertainty – or non-climatological variability – in the data. In the case of very high SNR, the observed values are retained in the mapped climatology and DIVA interpolates between them, while smaller values allow for larger deviations from these and an increasingly smooth climatology.

Working with real world observations, we know that the observations are indeed affected by shorter term variations and in addition have uncertainties associated with them. They do not represent the "true" climatological value. For this reason the SNR should always be kept quite small when making mapped climatologies, but this needs to be balanced by the need to keep the error estimates reasonable. The lower the SNR the further the approximation is allowed to deviate to be from the original data and the higher the error associated with the approximation becomes. The SNR can be calculated from observations using generalized cross validation, but for GLODAPv2 such calculations give very high SNR (in the order of 100). This is maybe not completely unreasonable, since GLODAPv2 has been carefully quality controlled and we have high confidence that the measurement uncertainties are small. Using gridded data covering 14 years as input also means that the input is reasonably representative relative to the climatology. However, both increasing the SNR and increasing the CL will decrease the error estimates, because this assumes small representativity errors (*i.e.* that what is observed is the true climatology) and a large circle of influence. If those assumptions are wrong the errors will be significantly underestimated. Therefore, even with a high confidence that the input data are climatologically representative the mapping errors are likely to be underestimated if we use the SNR calculated from general cross validation.

A DIVA analysis is created by minimizing a cost function which is defined by the difference between observations and analysis; the smoothness of the analysis; and the physical laws of the ocean (Troupin et al., 2012). The result is thus the analysis with the smallest global mean error, but determining the spatial distribution of errors is important. In

Earth Syst. Sci. Data Discuss., doi:10.5194/essd-2015-43, 2016
Manuscript under review for journal Earth Syst. Sci. Data
Published: 19 January 2016

DIVA this is non-trivial as, in contrast to OI, the real covariance function, which is necessary to obtain spatial error fields, is not formulated explicitly, but is instead the result of a numerical determination (Troupin et al., 2012). Determining the real covariance to get error estimates is the most exact method, but is computationally expensive. There are several error estimation methods implemented in DIVA, from the very simple to the very exact (Troupin et al., 2012, Beckers et al., 2014) and for GLODAPv2 the error fields are based on the "almost exact error calculation". This method calculates the exact error, using real covariances, in a few locations and then uses DIVA to interpolate between them. While not tested for all climatologies due to the significant computational cost, the almost exact errors generally only differ significantly from the exact error in regions where the data fields have very high errors, which only happens in coastal areas and in areas with no data. Since a mask removing the result in all grid cells where the mapping error exceeds one standard deviation in the input data (on a given pressure surface) have been applied to the mapped climatologies, the almost exact errors are considered equivalent to the real covariance errors.

3 Results

3.1 Data fields

The mapped climatologies are available as one netcdf files per parameter from CDIAC (http://cdiac.ornl.gov/oceans/GLODAPv2/). Each of these contain the global 1°x1° climatology, the associated error fields, and the gridded input data (Table 2) for the parameter in question. The files containing TCO_2, pH, Ω_C, and Ω_A are four-dimensional due to the two different time periods (1986-1999 and 2000-2013) for the top 1000 dbar. For all surfaces below 1000 dbar (*i.e.* surfaces 20-33) the TCO_2, pH, Ω_C, and Ω_A climatologies are identical for both time periods. The fields for the other parameters are three-dimensional, since the full time period 1972-2013 was used in the mapping.

Figures 2-4 show the mapped climatologies for TCO_2, TAlk, and nitrate, respectively, at two different pressure surfaces. These all show the spatial patterns expected from biological dynamics, global ocean salinity, and large-scale circulation. Figures 5-7 show, for the same parameters and pressure surfaces, the difference between the gridded input and the mapped climatologies, which is relatively large and variable near the surface and generally within the data uncertainties in the deep ocean. Figures 8-10 show the error fields associated with the climatologies shown in Figures 2-4. There are large differences in spatial data coverage

Earth Syst. Sci. Data Discuss., doi:10.5194/essd-2015-43, 2016
Manuscript under review for journal Earth Syst. Sci. Data
Published: 19 January 2016

between the 1986-1999 and the 2000-2013 periods (Figure 1), which affect the error estimates for the top 1000 dbar (Figure 8). The 1986-1999 period (Figure 1a) has no data in the Caribbean and Mediterranean Seas, and whereas the 2000-2013 period (Figure 1b) has data in those regions it lacks coverage in the Indian Ocean and has lower data density in the Pacific Ocean. The spatial variability in mapping errors is a function of the observational network, and further study of this variability would be of great use in optimizing the existing and future observational networks. The biggest improvement in GLODAPv2 compared to GLODAPv1.1 is that the former includes the Arctic Ocean and Mediterranean Sea which was missing in GLODAPv1.1 due to a near total absence of data from these regions.

3.2 Error fields

While the mapping error reflects the data distribution and the choice of input variables (*i.e.* CL and SNR), it represents only the errors due to the mathematical mapping of the input data, and does not take into account all the uncertainty in the input data (although some of this uncertainty is assumed in the choice of SNR). For details regarding the accuracy and precision of the GLODAPv2 discrete data the reader is referred to Olsen et al., (2015), but note that these uncertainties in the input data overall are smaller than the mapping errors. Overall the spatial error distribution is as expected: relatively small where there are observations and larger elsewhere. In regions without data the mapping errors may approach, and sometimes exceed, the climatological value. In these regions the climatology cannot be trusted, and therefore all grid cells where the mapping error exceeds one standard deviation of the input data on a given pressure surface have been masked (*i.e.* set to -999). This still leaves regions with high mapping errors, so the relative error fields (*i.e.* error scaled to the standard deviation in the data) are provided in the netcdf files making it possible for the user to create alternative masks if needed. For TCO_2 the average error in the masked data across all surfaces is in the range 14-27 μmol kg^{-1}; for TAlk in the range 8-29 μmol kg^{-1}; for pH at standard temperature and pressure in the range 0.016-0.056; for pH at *in situ* temperature and pressure in the range 0.011-0.042; for Ω_C at *in situ* temperature and pressure in the range 0.029-0.46; for Ω_A at *in situ* temperature and pressure in the range 0.020-0.31; for nitrate in the range 1.5-2.4 μmol kg^{-1}; for phosphate in the range 0.10-0.17 μmol kg^{-1}; for silicate in the range 4-13 μmol kg^{-1}; for oxygen in the range 10-19 μmol kg^{-1}; for salinity in the range 0.02-0.48; and for potential temperature in the range 0.19-2.5 ºC. The ranges reflect the variability in data density on

Earth Syst. Sci. Data Discuss., doi:10.5194/essd-2015-43, 2016
Manuscript under review for journal Earth Syst. Sci. Data
Published: 19 January 2016

289 different surfaces and also the larger variability in surface ocean observations, because this
290 leads to larger background variance in the input data.

291 The TCO_2 and TAlk mapping errors for our GLODAPv2 climatology have been
292 compared with those of GLODAPv1.1 (Figures 11-12). Note, however, that here we compare
293 pressure surfaces with depth surfaces. The most obvious result is the large spatial variability
294 in the differences, which seem to correlate with the data distribution. Very generally, there are
295 large differences (>10 μmol kg^{-1}) in error estimates between the GLODAPv2 2000-2013
296 TCO_2 climatology and the GLODAPv1.1 climatology (Figure 11b), and between the
297 GLODAPv2 1986-1999 and GLODAPv1.1 TCO2 climatologies in the top 200 dbar of the
298 Southern Ocean (exemplified by the 10 dbar surface in Figure 11a and 11b). In both cases the
299 error estimate in GLODAPv2 is frequently more than 15 μmol kg^{-1} higher than in
300 GLODAPv1.1. For TCO_2 the 1986-1999 climatology has comparable error to GLODAPv1.1
301 in the Atlantic, but is smaller by 10-15 μmol kg^{-1} in the Pacific (Figure 11a). For the 2000-
302 2013 TCO_2 climatology the GLODAPv2 mapping errors are frequently larger than those in
303 GLODAPv1.1, but here also smaller in the Pacific Ocean (Figure 11b). Below 1000 dbar
304 (exemplified by the 3000 dbar surface in Figure 11c) the mapping errors are overall larger by
305 5-10 μmol kg^{-1} in GLODAPv2 than in GLODAPv1.1. For TAlk the GLODAPv2 mapping
306 errors exceed those of GLODAPv1.1 in the Southern Ocean in the top 200 dbar (exemplified
307 by the 10 dbar surface in Figure 12a), but otherwise for the top 1000 dbar errors in the two
308 products are comparable (not shown). Below 1000 dbar the GLODAPv2 TAlk errors are
309 typically 5-10 μmol kg^{-1} larger than those of GLODAPv1.1 (exemplified by the 3000 dbar
310 surface in Figure 12b).

311 A scientific study of the differences in mapping error between GLODAPv1.1 and
312 GLODAPv2 and the mechanisms behind these would be worthwhile, and could perhaps
313 improve future climatologies of the marine CO_2 chemistry, but is beyond the scope of this
314 paper. The reasons for the differences seen in Figures 11-12 are currently not clear, but
315 several things are likely to contribute: (i) differences in the methods used; (ii) in general
316 GLODAPv2 uses a smaller CL and this results in larger errors, but for TCO_2 and pH in the
317 top 1000 dbar the CL is larger and this explains the smaller errors on these surfaces; (iii) there
318 are differences in data density and data distribution between the two versions, and the
319 improved distribution in GLODAPv2 leads to larger natural variability and thus larger, more
320 realistic, errors.

Earth Syst. Sci. Data Discuss., doi:10.5194/essd-2015-43, 2016
Manuscript under review for journal Earth Syst. Sci. Data
Published: 19 January 2016

For the macronutrients (nitrate, phosphate, silicate) the GLODAPv2 climatologies can be compared to the World Ocean Atlas (WOA) nutrient climatologies, but before doing so several things need to be considered: (i) methods used for mapping WOA (Garcia et al., 2010) are very different from those used in GLODAPv2; (ii) WOA also does not provide mapped error estimates for their climatologies; (iii) WOA reports nutrients with units μmol L^{-1} while GLODAPv2 uses units μmol kg^{-1}. Given the lack of error fields in WOA a direct comparison of errors like we did for TCO_2 and TAlk cannot be performed for the nutrients. Instead we have looked at the differences between the nitrate climatology in GLODAPv2 and in WOA09 (for the purpose of this comparison roughly converted the μmol L^{-1} data in WOA to μmol kg^{-1} by dividing by 1.024). These differences will be due to a combination of the differences in input data and the differences in mapping methods, and also here we compare pressure surfaces with depth surfaces. When comparing the GLODAPv2 gridded observations with the WOA09 climatology we see certain patterns (Figure 13). Near the surface the GLODAPv2 observations are overall smaller than the WOA09 climatology in high latitudes (Figure 13a), and this is most likely a manifestation of the seasonal bias in GLODAPv2 which in these regions contains almost only summertime data. In the tropics and subtropics the differences are within the data uncertainties. In the deep ocean (Figure 13b), however, the differences between the GLODAPv2 observations and the WOA09 climatology are very similar to the differences between the GLODAPv2 observations and climatology (Figure 7b). This suggests that below the seasonally influenced surfaces the differences between GLODAPv2 and WOA09 stem mainly from differences in mapping method, but that the climatologies otherwise are comparable. The biggest difference between GLODAPv2 and WOA09 is that the latter has considerably more input data, and is thus able to provide monthly climatologies which GLODAPv2 cannot. Note that we have compared the GLODAPv2 nitrate climatology to WOA09 since the WOA13 has a very different vertical resolution.

4 Best practices for using the GLODAPv2 1ºx1º data fields

For the marine CO_2 chemistry parameters with known, large, temporal trends two climatologies are provided for the surface ocean (<1000 dbar). This division was implemented to reduce the risk of converting time trends into spatial variations in the climatology. Alternative and more sophisticated approaches certainly exist, and these will be considered for future versions; here, however, we choose as simple and transparent an approach as possible. The 1986-1999 climatology is centered on the early 1990s and the

Earth Syst. Sci. Data Discuss., doi:10.5194/essd-2015-43, 2016
Manuscript under review for journal Earth Syst. Sci. Data
Published: 19 January 2016

2000-2013 climatology on the mid-2000s. The difference between the climatologies for the two time periods in no way represents an estimate of decadal change in global ocean CO_2. The errors in each TCO_2 climatology, mainly a consequence of limited spatial coverage of the input data, approach 100 μmol kg^{-1} in some regions, which is much larger than any expected trends. Additionally, each climatology was created using data from more than ten years, hence some fraction of our spatial features is a consequence of time trends in each of these periods. Users interested in time trends are better served by evaluating differences between repeat sections in the data product.

Planned future work includes creating mapped climatologies of several additional parameters available in the GLODAPv2 data product: water ages based on the halogenated transient tracer data and the ^{14}C data. As estimates of the anthropogenic CO_2 content based on the GLODAPv2 product become available we will consider creating new climatologies for TCO_2 and pH, where the anthropogenic trend in the data has been removed.

Acknowledgements

The work of S. K. Lauvset was funded by the Norwegian Research Council through the projects DECApH (214513/F20). The EU-IP CARBOCHANGE (FP7 264878) provided funding for A. Olsen, S. van Heuven, T. Tanhua, R. Steinfeldt, as well as the project framework that instigated GLODAPv2. A. Olsen additionally acknowledges generous support from the FRAM - High North Research Centre for Climate and the Environment, the Centre for Climate Dynamics at the Bjerknes Centre for Climate Research, the EU AtlantOS (grant agreement No 633211) project and the Norwegian Research Council project SNACS (229752). A. Kozyr acknowledges funding from the US Department of Energy. M. Ishii acknowledges the project MEXT 24121003. A. Velo and F. F. Pérez were supported by BOCATS (CTM20134410484P) project cofounded by the Spanish Government and the Fondo Europeo de Desarrollo Regional (FEDER). The International Ocean Carbon Coordination Project (IOCCP) partially supported this activity through the U.S. National Science Foundation grant (OCE- 1243377) to the Scientific Committee on Oceanic Research.

"The research leading to the last developments of DIVA has received funding from the European Union Seventh Framework Programme (FP7/2007-2013) under grant agreement No. 283607, SeaDataNet 2, and from the project EMODNET (MARE/2012/10 - Lot 4 Chemistry - SI2.656742) from the Directorate-General for Maritime Affairs and Fisheries."

Earth Syst. Sci. Data Discuss., doi:10.5194/essd-2015-43, 2016
Manuscript under review for journal Earth Syst. Sci. Data
Published: 19 January 2016

Open Access Earth System Science Data Discussions

References

Bakker, D. C. E., Pfeil, B., Smith, K., Hankin, S., Olsen, A., Alin, S. R., Cosca, C., Harasawa, S., Kozyr, A., Nojiri, Y., O'Brien, K. M., Schuster, U., Telszewski, M., Tilbrook, B., Wada, C., Akl, J., Barbero, L., Bates, N. R., Boutin, J., Bozec, Y., Cai, W. J., Castle, R. D., Chavez, F. P., Chen, L., Chierici, M., Currie, K., de Baar, H. J. W., Evans, W., Feely, R. A., Fransson, A., Gao, Z., Hales, B., Hardman-Mountford, N. J., Hoppema, M., Huang, W. J., Hunt, C. W., Huss, B., Ichikawa, T., Johannessen, T., Jones, E. M., Jones, S. D., Jutterström, S., Kitidis, V., Körtzinger, A., Landschützer, P., Lauvset, S. K., Lefèvre, N., Manke, A. B., Mathis, J. T., Merlivat, L., Metzl, N., Murata, A., Newberger, T., Omar, A. M., Ono, T., Park, G. H., Paterson, K., Pierrot, D., Ríos, A. F., Sabine, C. L., Saito, S., Salisbury, J., Sarma, V. V. S. S., Schlitzer, R., Sieger, R., Skjelvan, I., Steinhoff, T., Sullivan, K. F., Sun, H., Sutton, A. J., Suzuki, T., Sweeney, C., Takahashi, T., Tjiputra, J., Tsurushima, N., van Heuven, S. M. A. C., Vandemark, D., Vlahos, P., Wallace, D. W. R., Wanninkhof, R., and Watson, A. J.: An update to the Surface Ocean CO2 Atlas (SOCAT version 2), Earth Syst. Sci. Data, 6, 69-90, 2014.

Beckers, J.-M., Barth, A., Troupin, C., and Alvera-Azcárate, A.: Approximate and Efficient Methods to Assess Error Fields in Spatial Gridding with Data Interpolating Variational Analysis (DIVA), Journal of Atmospheric and Oceanic Technology, 31, 515-530, 2014.

Bopp, L., Resplandy, L., Orr, J. C., Doney, S. C., Dunne, J. P., Gehlen, M., Halloran, P., Heinze, C., Ilyina, T., Seferian, R., Tjiputra, J., and Vichi, M.: Multiple stressors of ocean ecosystems in the 21st century: projections with CMIP5 models, Biogeosciences, 10, 6225-6245, 2013.

Dickson, A.: Standard potential of the reaction: AgCl (s) + 1/2H_2(g) = Ag (s) + HCl (aq), and the standard acidity constant of the ion HSO_4^- in synthetic sea water from 273.15 to 318.15 K, J. Chem. Thermodyn., 22, 113–127, 1990.

Feely, R., Talley, L., Bullister, J. L., Carlson, C. A., Doney, S., Fine, R. A., Firing, E., Gruber, N., Hansell, D. A., Johnson, G. C., Key, R., Langdon, C., Macdonald, A., Mathis, J., Mecking, S., Millero, F. J., Mordy, C., Sabine, C., Smethie, W. M., Swift, J. H., Thurnherr, A. M., Wanninkhof, R., and Warner, M.: The US Repeat Hydrography CO2/Tracer Program (GO-SHIP): Accomplishments from the first decadal survey, US CLIVAR and OCB Report 2014-5, US CLIVAR Project Office, 47 pp., 2014.

Garcia, H. E., Locarnini, R. A., Boyer, T. P., Antonov, J. I., Zweng, M. M., Baranova, O. K., and Johnson, D. R.: World Ocean Atlas 2009, Volume 4: Nutrients (phosphate, nitrate, silicate). S. Levitus, Ed., NOAA Atlas NESDIS 71, U.S. Government Printing Office, Washington, D.C., 398 pp pp., 2010.

Gouretski, V. V. and Jancke, K.: Systematic errors as the cause for an apparent deep water property variability: global analysis of the WOCE and historical hydrographic data, Progress in Oceanography, 48, 337-402, 2001.

Johnson, G. C., Robbins, P. E., and Hufford, G. E.: Systematic adjustments of hydrographic sections for internal consistency, Journal of Atmospheric and Oceanic Technology, 18, 1234-1244, 2001.

Jones, S. D., Le Quéré, C., and Rödenbeck, C.: Autocorrelation characteristics of surface ocean pCO2 and air-sea CO2 fluxes, Global Biogeochem. Cycles, 26, GB2042, 2012.

Key, R. M., Kozyr, A., Sabine, C. L., Lee, K., Wanninkhof, R., Bullister, J. L., Feely, R. A., Millero, F. J., Mordy, C., and Peng, T. H.: A global ocean carbon climatology: Results from Global Data Analysis Project (GLODAP), Global Biogeochemical Cycles, 18, GB4031, doi:10.1029/2004GB002247, 2004.

436 Key, R. M., Tanhua, T., Olsen, A., Hoppema, M., Jutterström, S., Schirnick, C., Van Heuven,
437 S., Kozyr, A., Lin, X., Velo, A., Wallace, D. W. R., and Mintrop, L.: The CARINA
438 data synthesis project: introduction and overview, Earth Syst. Sci. Data, 2, 105-121,
439 2010.
440 Lauvset, S. K., Gruber, N., Landschützer, P., Olsen, A., and Tjiputra, J.: Trends and drivers in
441 global surface ocean pH over the past 3 decades, Biogeosciences, 12, 1285-1298,
442 2015.
443 Levitus, S., and Boyer, T.P.: World Ocean Atlas, vol. 4, Temperature, NOAA Atlas NESDIS
444 4, National Oceanic and Atmospheric Administration, Silver Spring, Md., 1994.
445 Lewis, E. and Wallace, D. W. R.: Program developed for CO2 system calculations. In:
446 ORNL/CDIAC-105, Carbon Dioxide Information Analysis Center, Oak Ridge
447 National Laboratory, U.S. Department of Energy, Oak Ridge, Tennessee, 1998.
448 Lueker, T. J., Dickson, A. G., and Keeling, C. D.: Ocean pCO(2) calculated from dissolved
449 inorganic carbon, alkalinity, and equations for K-1 and K-2: validation based on
450 laboratory measurements of CO2 in gas and seawater at equilibrium, Marine
451 Chemistry, 70, 105-119, 2000.
452 Olsen, A., Key, R. M., Lauvset, S. K., Van Heuven, S., Lin, X., Schirnick, C., Tanhua, T.,
453 Hoppema, M., Jutterström, S., Steinfeldt, R., Jeansson, E., Ishii, M., Suzuki, T., Velo,
454 A., Pfeil, B., and Kozyr, A.: Building a fully consistent carbon-relevant data product
455 for the world ocean: the Global Ocean Data Project, version 2 (GLODAPv2),
456 *submitted to:* Earth Syst. Sci. Data Discuss., 2015.
457 Orr, J. C., Maier-Reimer, E., Mikolajewicz, U., Monfray, P., Sarmiento, J. L., Toggweiler, J.
458 R., Taylor, N. K., Palmer, J., Gruber, N., Sabine, C. L., Le Quéré, C., Key, R. M., and
459 Boutin, J.: Estimates of anthropogenic carbon uptake from four three-dimensional
460 global ocean models, Global Biogeochemical Cycles, 15, 43-60, 2001.
461 Pfeil, B., Olsen, A., Bakker, D. C. E., Hankin, S., Koyuk, H., Kozyr, A., Malczyk, J., Manke,
462 A., Metzl, N., Sabine, C. L., Akl, J., Alin, S. R., Bates, N., Bellerby, R. G. J., Borges,
463 A., Boutin, J., Brown, P. J., Cai, W. J., Chavez, F. P., Chen, A., Cosca, C., Fassbender,
464 A. J., Feely, R. A., González-Dávila, M., Goyet, C., Hales, B., Hardman-Mountford,
465 N., Heinze, C., Hood, M., Hoppema, M., Hunt, C. W., Hydes, D., Ishii, M.,
466 Johannessen, T., Jones, S. D., Key, R. M., Körtzinger, A., Landschützer, P., Lauvset,
467 S. K., Lefèvre, N., Lenton, A., Lourantou, A., Merlivat, L., Midorikawa, T., Mintrop,
468 L., Miyazaki, C., Murata, A., Nakadate, A., Nakano, Y., Nakaoka, S., Nojiri, Y.,
469 Omar, A. M., Padin, X. A., Park, G. H., Paterson, K., Perez, F. F., Pierrot, D., Poisson,
470 A., Ríos, A. F., Santana-Casiano, J. M., Salisbury, J., Sarma, V. V. S. S., Schlitzer, R.,
471 Schneider, B., Schuster, U., Sieger, R., Skjelvan, I., Steinhoff, T., Suzuki, T.,
472 Takahashi, T., Tedesco, K., Telszewski, M., Thomas, H., Tilbrook, B., Tjiputra, J.,
473 Vandemark, D., Veness, T., Wanninkhof, R., Watson, A. J., Weiss, R., Wong, C. S.,
474 and Yoshikawa-Inoue, H.: A uniform, quality controlled Surface Ocean CO2 Atlas
475 (SOCAT), Earth Syst. Sci. Data, 5, 125-143, 2013.
476 Rixen, M., Beckers, J. M., Brankart, J. M., and Brasseur, P.: A numerically efficient data
477 analysis method with error map generation, Ocean Model., 2, 45-60, 2000.
478 Sabine, C. L., Feely, R. A., Gruber, N., Key, R. M., Lee, K., Bullister, J. L., Wanninkhof, R.,
479 Wong, C. S., Wallace, D. W. R., Tilbrook, B., Millero, F. J., Peng, T.-H., Kozyr, A.,
480 Ono, T., and Ríos, A. F.: The oceanic sink for anthropogenic CO_2, Science, 305, 367-
481 371, 2004.
482 Sabine, C. L., Hankin, S., Koyuk, H., Bakker, D. C. E., Pfeil, B., Olsen, A., Metzl, N., Kozyr,
483 A., Fassbender, A., Manke, A., Malczyk, J., Akl, J., Alin, S. R., Bellerby, R. G. J.,
484 Borges, A., Boutin, J., Brown, P. J., Cai, W. J., Chavez, F. P., Chen, A., Cosca, C.,
485 Feely, R. A., González-Dávila, M., Goyet, C., Hardman-Mountford, N., Heinze, C.,

Hoppema, M., Hunt, C. W., Hydes, D., Ishii, M., Johannessen, T., Key, R. M., Körtzinger, A., Landschützer, P., Lauvset, S. K., Lefèvre, N., Lenton, A., Lourantou, A., Merlivat, L., Midorikawa, T., Mintrop, L., Miyazaki, C., Murata, A., Nakadate, A., Nakano, Y., Nakaoka, S., Nojiri, Y., Omar, A. M., Padin, X. A., Park, G. H., Paterson, K., Perez, F. F., Pierrot, D., Poisson, A., Ríos, A. F., Salisbury, J., Santana-Casiano, J. M., Sarma, V. V. S. S., Schlitzer, R., Schneider, B., Schuster, U., Sieger, R., Skjelvan, I., Steinhoff, T., Suzuki, T., Takahashi, T., Tedesco, K., Telszewski, M., Thomas, H., Tilbrook, B., Vandemark, D., Veness, T., Watson, A. J., Weiss, R., Wong, C. S., and Yoshikawa-Inoue, H.: Surface Ocean CO2 Atlas (SOCAT) gridded data products, Earth Syst. Sci. Data, 5, 145-153, 2013.

Sabine, C. L. and Tanhua, T.: Estimation of Anthropogenic CO2 Inventories in the Ocean, Annual Review of Marine Science, 2, 175-198, 2010.

Suzuki, T., Ishii, M., Aoyama, M., Christian, J. R., Enyo, K., Kawano, T., Key, R. M., Kosugi, N., Kozyr, A., Miller, L., Murata, A., Nakano, T., Ono, T., Saino, T., Sasaki, K.-I., Sasano, D., Takatani, Y., Wakita, M., and Sabine, C.: PACIFICA Data Synthesis Project, Carbon Dioxide Information Analysis Center, Oak Ridge National Laboratory, U.S. Department of Energy, Oak Ridge, Tennessee, 2013.

Talley, L. D., Feely, R. A., Sloyan, B. M., Wanninkhof, R., Baringer, M. O., Bullister, J. L., Carlson, C. A., Doney, S. C., Fine, R. A., Firing, E., Gruber, N., Hansell, D. A., Ishii, M., Johnson, G. C., Katsumata, K., Key, R. M., Kramp, M., Langdon, C., Macdonald, A. M., Mathis, J. T., McDonagh, E. L., Mecking, S., Millero, F. J., Mordy, C. W., Nakano, T., Sabine, C. L., Smethie, W. M., Swift, J. H., Tanhua, T., Thurnherr, A. M., Warner, M. J., and Zhang, J.-Z.: Changes in Ocean Heat, Carbon Content, and Ventilation: A Review of the First Decade of GO-SHIP Global Repeat Hydrography, *Annual Review of Marine Science*, 8, null, doi:10.1146/annurev-marine-052915-100829, 2016.

Touratier, F., Azouzi, L., and Goyet, C.: CFC-11, Delta C-14 and H-3 tracers as a means to assess anthropogenic CO2 concentrations in the ocean, Tellus Series B-Chemical and Physical Meteorology, 59, 318-325, 2007.

Troupin, C., Barth, A., Sirjacobs, D., Ouberdous, M., Brankart, J. M., Brasseur, P., Rixen, M., Alvera-Azcárate, A., Belounis, M., Capet, A., Lenartz, F., Toussaint, M. E., and Beckers, J. M.: Generation of analysis and consistent error fields using the Data Interpolating Variational Analysis (DIVA), Ocean Model., 52–53, 90-101, 2012.

Uppstrom, L. R.: Boron/chlorinity ratio of deep-sea water from the Pacific Ocean, Deep-Sea Research, 21, 161-162, 1974.

van Heuven, S., Pierrot, D., Lewis, E., and Wallace, D.: MATLAB Program developed for CO_2 system calculations, ORNL/CDIAC-105b, Carbon Dioxide Information Analysis Center, Oak Ridge National Laboratory, US Department of Energy, Oak Ridge, Tennessee, 2009.

Tables

Table 1. Maximum distance criteria used when vertically interpolating the input data.

Range (dbar)	Maximum distance allowed
0–200.99	100
201–750.99	200
751–1500.99	250
1501–12000	500

Earth Syst. Sci. Data Discuss., doi:10.5194/essd-2015-43, 2016
Manuscript under review for journal Earth Syst. Sci. Data
Published: 19 January 2016

Open Access Earth System Science Data Discussions

529 **Table 2. List of information available in the netcdf data files.**

Variable name	Description
lon	Longitude in degrees east, range -180 – 180
lat	Latitude in degrees north, range -90 – 90
tco2, talk, pH, Ω_C, Ω_A, nitrate, phosphate, silicate, oxygen, salinity, theta	Mapped climatology with land mask and 3σ mask applied.
_error	Mapping error associated with the mapped climatology
_relerr	Mapping error scaled with the global standard deviation of the input data
Input_mean	Binned and averaged mean of the observations on the same grid as the climatology
Input_std	Standard deviation of the binned mean.
Input_N	Number of observational data points in the grid cell
Input_lon	Binned and averaged longitude in degrees east
Input_lat	Binned and averaged latitude in degrees north

530

531 ## Figures

532 **Figure 1. a) Data density of TCO_2 in the years 1986-1999; b) Data density of TCO_2 in the years 2000-2013.**
533 **Both figures show data at the 10 dbar surface.**

534 **Figure 2. Mapped climatology of TCO_2 at 10 dbar (a, b) and 3000 dbar (c). a) is the climatology for the**
535 **1986-1999 period while b) is for the 2000-2013 period.**

536 **Figure 3. Mapped climatology of TAlk at 10 dbar (a) and 3000 dbar (b).**

537 **Figure 4. Mapped climatology of nitrate at 10 dbar (a) and 3000 dbar (b).**

538 **Figure 5. Difference between the gridded TCO_2 input data and the mapped climatologies atv10 dbar (a,b)**
539 **and 3000 dbar (c). a) is the climatology for the 1986-1999 period while b) is for the 2000-2013 period.**

540 **Figure 6. Difference between the gridded TAlk input data and the mapped climatologies at 10 dbar (a)**
541 **and 3000 dbar (b).**

542 **Figure 7. Difference between the gridded nitrate input data and the mapped climatologies at 10 dbar (a)**
543 **and 3000 dbar (b).**

544 **Figure 8. Mapping error for TCO_2 at 10 dbar (a, b) and 3000 dbar (c). a) is the error for the 1986-1999**
545 **climatology while b) is for the 2000-2013 climatology. Notice how the error is large between repeat**
546 **transect and creates a spatial pattern of square-like features in the Pacific.**

547 **Figure 9. Mapping error for TAlk at 10 dbar (a) and 3000 dbar (b). Notice how the error is large between**
548 **repeat transect and creates a spatial pattern of square-like features in the Pacific.**

549 **Figure 10. Mapping error for nitrate at 10 dbar (a) and 3000 dbar (b). Notice how the error is large**
550 **between repeat transect and creates a spatial pattern of square-like features in the Pacific.**

551 **Figure 11. Difference in error estimates for TCO_2 between GLODAPv2 and GLODAPv1.1. a) compares**
552 **the 10 dbar surface from the 1986-1999 climatology in v2 with the 10 m surface in v1.1; b) compares the**
553 **10 dbar surface from the 2000-2013 climatology in v2 with the 10 m surface in v1.1; c) compares the 3000**
554 **dbar surface in v2 with the 3000 m surface in v1.1.**

Earth Syst. Sci. Data Discuss., doi:10.5194/essd-2015-43, 2016
Manuscript under review for journal Earth Syst. Sci. Data
Published: 19 January 2016

Open Access Earth System Science Data Discussions

555 **Figure 12. Difference in error estimates for TAlk between GLODAPv2 and GLODAPv1.1. a) compares**
556 **the 10 dbar surface in v2 with the 10 m surface in v1.1, while b) compares the 3000 dbar surface in v2 with**
557 **the 3000 m surface in v1.1.**

558 **Figure 13. Differences between the GLODAPv2 nitrate gridded input data and the WOA09 annual**
559 **mapped nitrate climatology. a) compares the 10 dbar surface in GLODAPv2 with the 10 m surface in**
560 **WOA09, while b) compares the 3000 dbar surface in GLODAPv2 with the 3000 m surface in WOA09.**

Earth Syst. Sci. Data Discuss., doi:10.5194/essd-2015-43, 2016
Manuscript under review for journal Earth Syst. Sci. Data
Published: 19 January 2016

Open Access Earth System Science Data Discussions

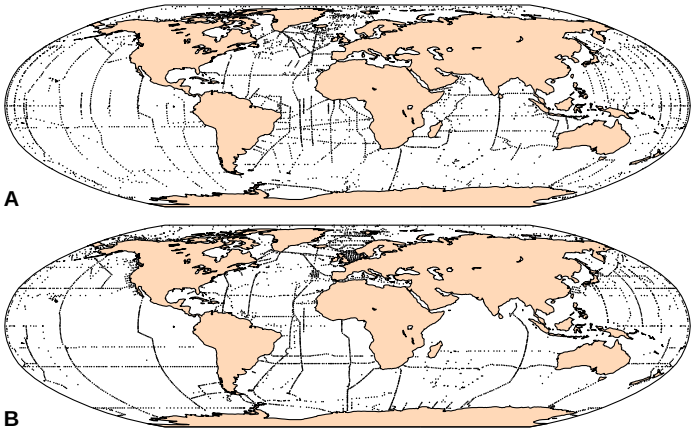

Fig. 1

Earth Syst. Sci. Data Discuss., doi:10.5194/essd-2015-43, 2016
Manuscript under review for journal Earth Syst. Sci. Data
Published: 19 January 2016

Open Access Earth System Science Data Discussions

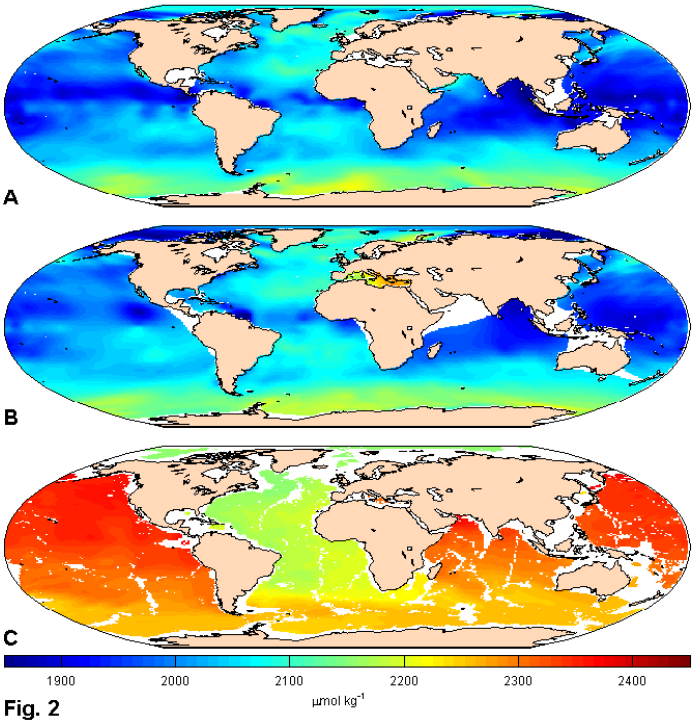

Fig. 2

Earth Syst. Sci. Data Discuss., doi:10.5194/essd-2015-43, 2016
Manuscript under review for journal Earth Syst. Sci. Data
Published: 19 January 2016

Open Access Earth System Science Data Discussions

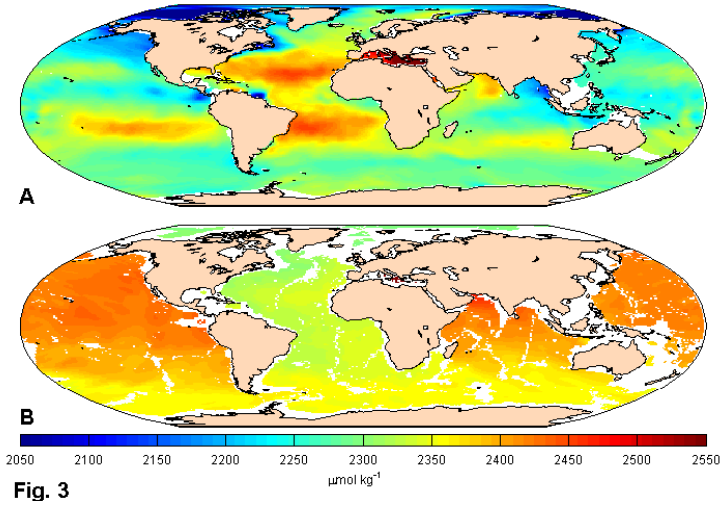

Fig. 3

Earth Syst. Sci. Data Discuss., doi:10.5194/essd-2015-43, 2016
Manuscript under review for journal Earth Syst. Sci. Data
Published: 19 January 2016

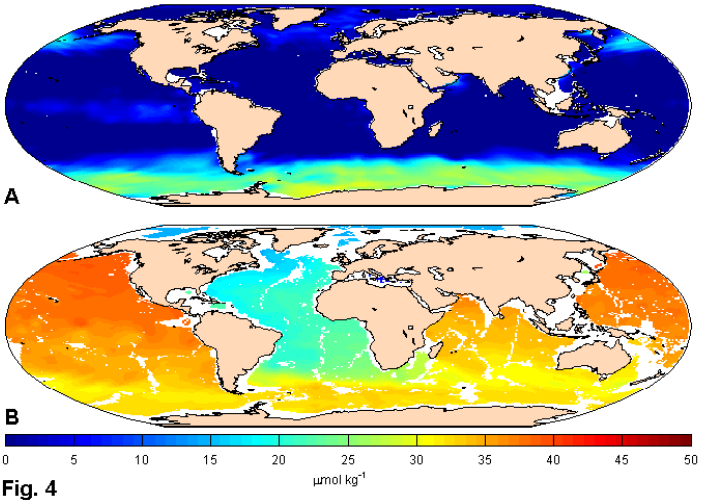

Fig. 4

Earth Syst. Sci. Data Discuss., doi:10.5194/essd-2015-43, 2016
Manuscript under review for journal Earth Syst. Sci. Data
Published: 19 January 2016

Open Access Earth System Science Data Discussions

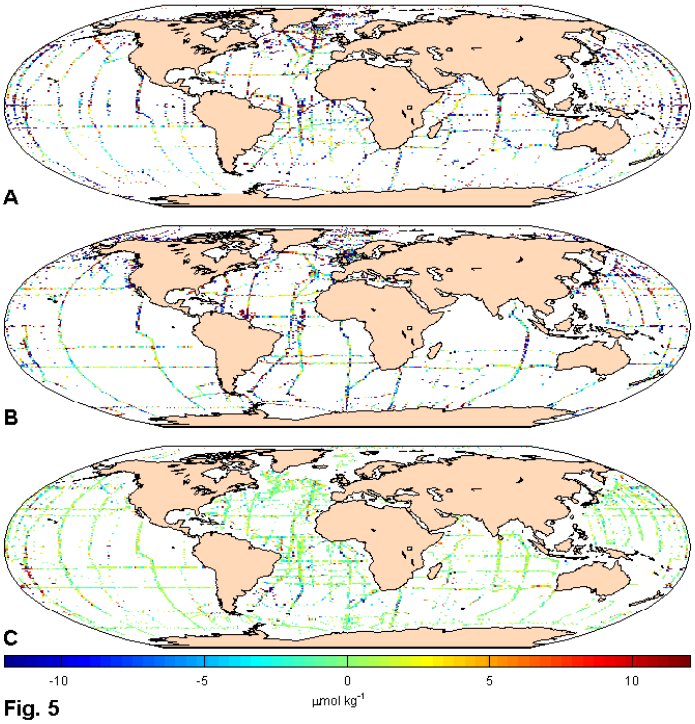

Fig. 5

Earth Syst. Sci. Data Discuss., doi:10.5194/essd-2015-43, 2016
Manuscript under review for journal Earth Syst. Sci. Data
Published: 19 January 2016

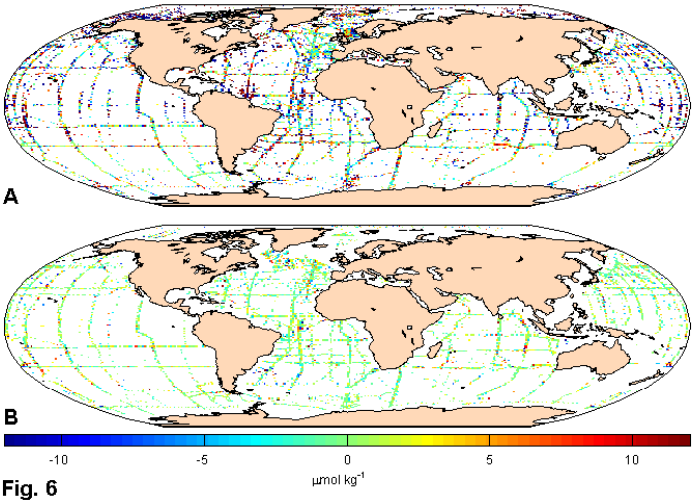

Fig. 6

Earth Syst. Sci. Data Discuss., doi:10.5194/essd-2015-43, 2016
Manuscript under review for journal Earth Syst. Sci. Data
Published: 19 January 2016

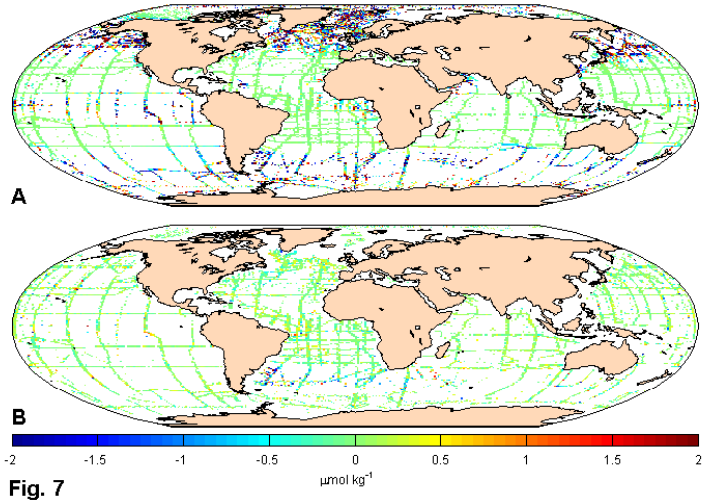

Fig. 7

Earth Syst. Sci. Data Discuss., doi:10.5194/essd-2015-43, 2016
Manuscript under review for journal Earth Syst. Sci. Data
Published: 19 January 2016

Open Access Earth System Science Data Discussions

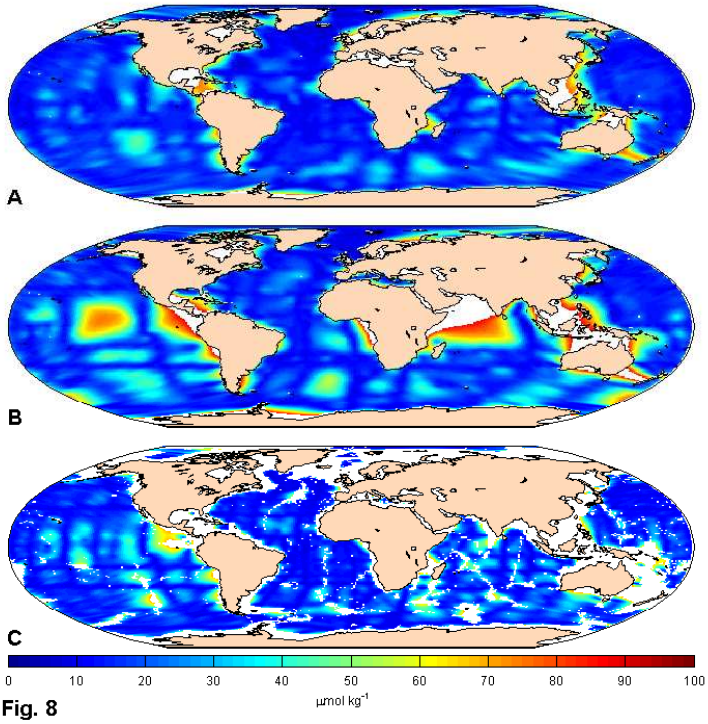

Fig. 8

Earth Syst. Sci. Data Discuss., doi:10.5194/essd-2015-43, 2016
Manuscript under review for journal Earth Syst. Sci. Data
Published: 19 January 2016

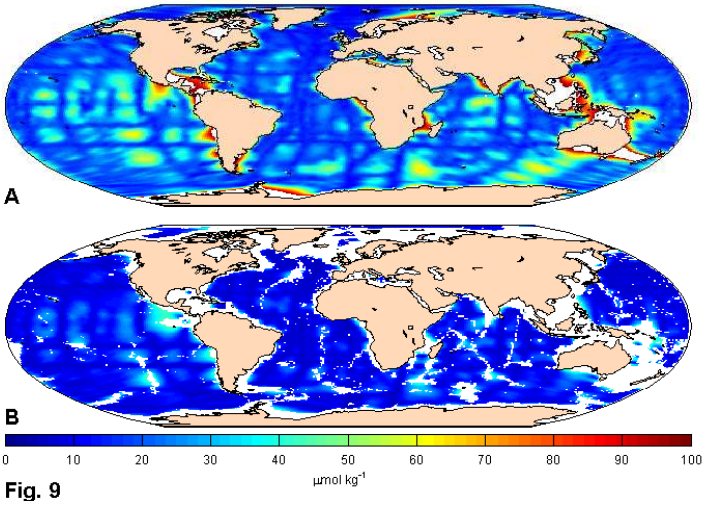

Fig. 9

Earth Syst. Sci. Data Discuss., doi:10.5194/essd-2015-43, 2016
Manuscript under review for journal Earth Syst. Sci. Data
Published: 19 January 2016

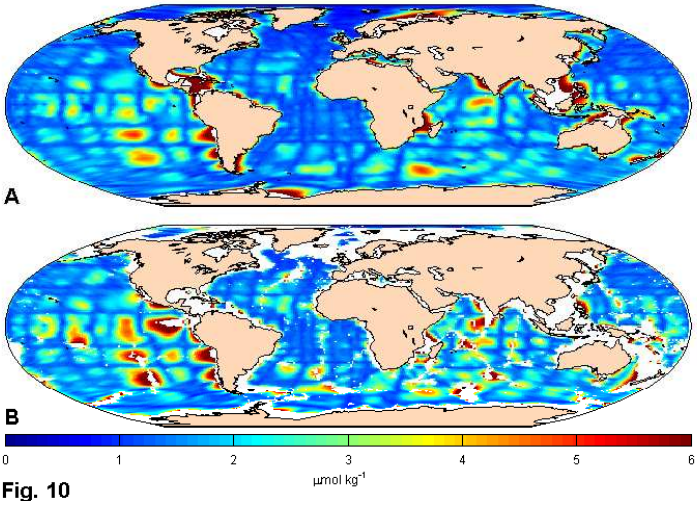

Fig. 10

Earth Syst. Sci. Data Discuss., doi:10.5194/essd-2015-43, 2016
Manuscript under review for journal Earth Syst. Sci. Data
Published: 19 January 2016

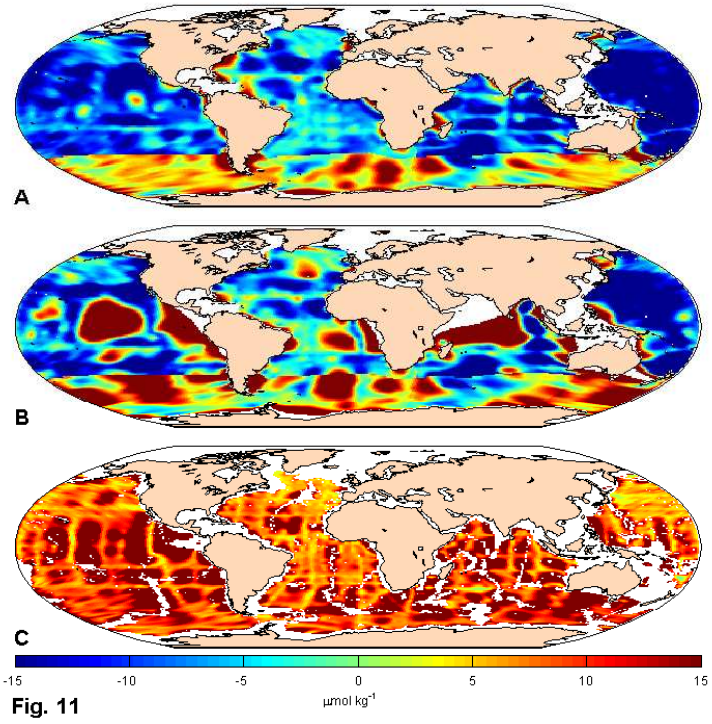

Fig. 11

Earth Syst. Sci. Data Discuss., doi:10.5194/essd-2015-43, 2016
Manuscript under review for journal Earth Syst. Sci. Data
Published: 19 January 2016

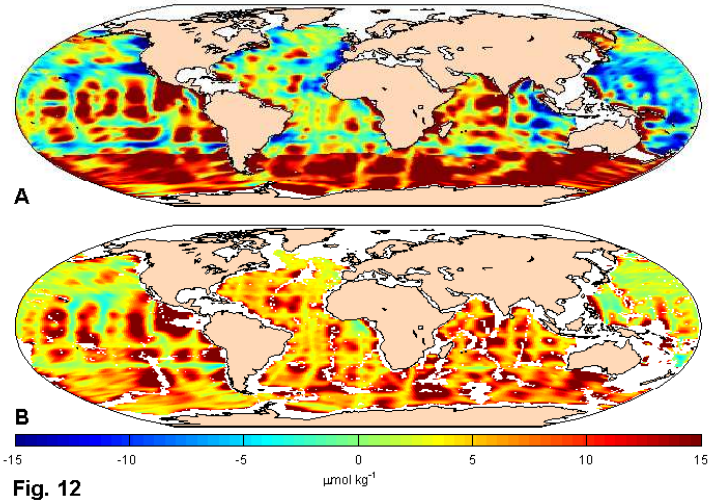

Fig. 12

Earth Syst. Sci. Data Discuss., doi:10.5194/essd-2015-43, 2016
Manuscript under review for journal Earth Syst. Sci. Data
Published: 19 January 2016

Open Access Earth System Science Data Discussions

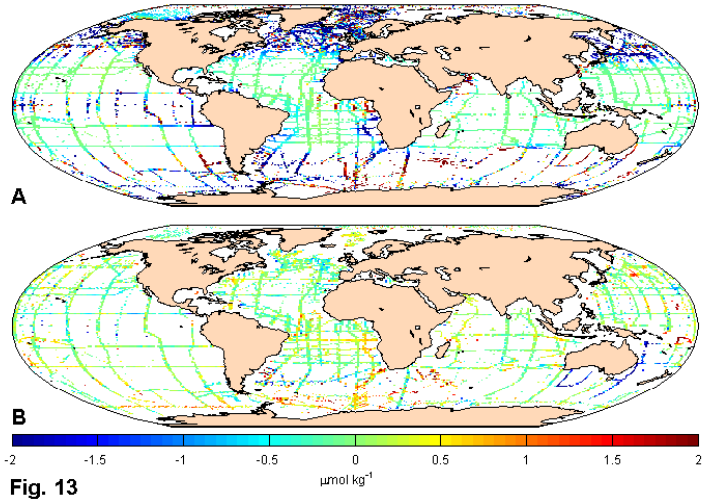

Fig. 13